The OSCAR PUBLISHING Services
American Journal of Applied Science and Technology

VOLUME Vol.06 Issue03 2026
PAGE NO. 183-200
DOI 10.37547/ajast/Volume06Issue03-28

Rising Atmospheric Demand and Water Stress in The Syr Darya River Basin: A GIS-Based Assessment Of 2000–2025 Trends and SSP Scenarios To 2035

Azizbek O. Hasanov

Independent Researcher, Research Institute of Environmental and Nature Protection Technologies under Central Asian University of Environmental and Climate Change Studies (Green University), Uzbekistan

Bakhtiyor A. Pulatov

Rector of Central Asian University of Environmental and Climate Change Studies (Green University), Doctor of Technical Sciences (DSc), Professor, Uzbekistan

Received: 12 February 2026; **Accepted:** 08 March 2026; **Published:** 31 March 2026

Abstract: The Syr Darya is Central Asia's main transboundary river shared by Kyrgyzstan, Uzbekistan, Tajikistan and Kazakhstan, yet basin-wide assessments that link climate, runoff, reservoir operation and water withdrawal in one spatial framework remain scarce. We built a harmonised hydroclimatic database for 2000–2025 and analysed it with Mann–Kendall, Sen's slope and Pettitt tests, SPI-12 and SPEI-12 drought indices, correlation and regularised regression, and GIS mapping in ArcGIS Pro. Near-term change to 2035 was estimated with a delta approach under SSP1-2.6, SSP2-4.5, SSP3-7.0 and SSP5-8.5. Mean annual air temperature rose by 0.0329 °C yr^{-1} ($p = 0.003$), with a change point around 2013, and potential evapotranspiration (PET) rose by 1.198 mm yr^{-1} ($p = 0.011$). Precipitation (317.65 mm) and basin runoff (37.95 km^3) showed no significant trend but strong interannual variability (runoff 27.64 km^3 in 2007 vs 50.29 km^3 in 2009). In the 2025 baseline, runoff was 33.25 km^3 (−12.38 %), withdrawal was almost unchanged at 13.33 km^3, and the withdrawal-to-runoff ratio reached 40.09 %. By 2035, runoff is projected at 37.85–36.48 km^3 (−0.25 % to −3.87 % relative to 2000–2024), snowfall declines by 8–16 % and summer climatic water balance falls to −506.42 mm under SSP5-8.5. Water-supply maps show a persistent upstream–downstream gradient, with the lower reaches and the summer irrigation season the most exposed. Water stress in the basin is therefore driven less by falling precipitation than by rising atmospheric demand acting on near-constant withdrawals.

Keywords: Syr Darya; climate change; water stress; GIS; SPEI; Mann–Kendall; SSP scenarios; Central Asia.

1. Introduction: Warming is changing how much water snow- and glacier-fed rivers deliver, and when they deliver it. Higher air temperatures raise evapotranspiration, shorten snow-cover duration and advance melt, so the share of runoff available in summer tends to fall even where annual totals hold steady [1, 2]. Mountain catchments that act as "water towers" for downstream lowlands are among the most sensitive and most depended-upon systems on Earth [3].

Central Asia is a clear case. The Tien Shan and Pamir-Alay ranges store water as snow and ice and release it to arid plains where rainfall alone cannot support agriculture or settlements [4, 5]. Glaciers in the Tien Shan have been shrinking, and the fraction of precipitation falling as snow is declining in alpine parts of the region [4, 6]. Glacier melt can temporarily raise runoff, but it passes a "peak water" point beyond which contributions decline as ice volume shrinks [2].

The Syr Darya basin concentrates these pressures.

Runoff forms mainly in Kyrgyzstan and Tajikistan, while most of it is used for irrigation in Uzbekistan and Kazakhstan [7, 8]. Large reservoirs such as Toktogul, Andijan, Bahri Tojik (Kairakkum), Charvak and Shardara redistribute flow between winter hydropower demand upstream and summer irrigation demand downstream [9, 10]. Earlier studies have shown that both climate and human activities shape the basin's runoff [11–13], projected changes for individual sub-catchments [14–16], and assessed water allocation and adaptation options [7, 17].

Most of this work, however, addresses one component at a time: glaciers, a single sub-basin, irrigation efficiency or groundwater. Few studies combine climate drivers, upstream inflow, basin runoff and total withdrawal for the whole transboundary basin in one consistent statistical and GIS framework. Fewer still separate a recent baseline year from the long-term mean and carry that baseline forward to near-term scenarios that water managers can use within a planning horizon.

This study addresses that gap for the Syr Darya basin. Its objectives were to:

1. build a harmonised hydroclimatic and water-use database for 2000–2025 and process it with consistent statistical and GIS methods;
2. quantify long-term trends, change points and drought conditions in temperature, precipitation, PET, climatic water balance, Toktogul inflow and basin runoff for 2000–2024;
3. map the spatio-temporal pattern of water supply across the upper, middle and lower basin and assess 2025 as a baseline year;
4. estimate meteorological conditions, runoff, withdrawal pressure and water-stress exposure to 2035 under four SSP scenarios.

2. METHODS

2.1. Study area

The Syr Darya forms at the confluence of the Naryn and Karadarya in the eastern Fergana Valley and flows north-west to the Aral Sea. Its length is about 3,019 km from the Naryn source and 2,212 km from the confluence; the hydrologically active catchment covers about 219,000 km² [18]. The Naryn (807 km, 59,100 km², about 14.5 km³ yr^{-1}) and Karadarya (177 km, 30,100 km², about 3.9 km³ yr^{-1}) supply most of the flow, and long-term basin water resources are reported at about 37.2 km³ yr^{-1} [18]. Toktogul, the largest reservoir, has a total capacity of 19.5 km³ and a live storage of 14 km³ [19].

For analysis the basin was divided into three zones (Fig. 1). The upper zone (Central and Western Tien Shan, Alay and Fergana ranges) is where runoff forms. The middle zone (Fergana Valley, Tashkent oasis, Mirzachul) regulates and redistributes water through reservoirs and canals. The lower zone (Turkestan and Kyzylorda plains, Syr Darya delta) depends almost entirely on inflow from upstream.



Fig. 1. Location of the Syr Darya River Basin and the study area.

2.2. Data and harmonisation

The database has three time blocks: a retrospective series (2000–2024), a baseline year (2025) and scenario values (2026–2035), stored separately so that observed and modelled values are never mixed. Data sources are listed in Table 1. Every record carries the year, indicator, spatial unit, unit of measure, source, processing method and a status flag, in line with WMO data-management guidance and the FAIR principles [26, 27].

Data group	Main indicators	Period, step	Source / status
Climate	Mean, min and max air temperature; precipitation; relative humidity; PET	2000–2025, monthly and annual	ERA5-Land and CRU TS v4 methodology [20, 21]; harmonised basin-scale series
Snow	Snowfall; maximum snow water equivalent	2000–2025, monthly and annual	MODIS snow products [22]; harmonised series
Hydrology	Toktogul inflow and outflow; annual balance; basin runoff	2000–2025, monthly and annual	Official and documented values; statistically reconstructed gaps [18, 19]
Water use	Total withdrawal; withdrawal-to-runoff ratio; water availability index	2000–2025, annual	Official water-management data, published estimates; reconstructed gaps

Data group	Main indicators	Period, step	Source / status
Relief and hydrography	Elevation, slope, flow direction, flow accumulation; rivers, reservoirs, sub-basins	Static	SRTM DEM [23]; HydroSHEDS [24]
Scenarios	Temperature, precipitation, PET, snowfall, runoff, withdrawal	2026–2035, annual	Delta-change scenarios (Section 2.5)

Table 1. Data used in the study.

Each value was flagged as observed, documented, calculated or reconstructed. Names, units and spatial codes were standardised, and records were screened for duplicates, physically impossible values and unexplained jumps; outliers were checked against known extreme events before any decision to keep or remove them [26].

Gaps in the historical basin runoff series were filled from its relationship with Toktogul inflow, using a logistic-bounded regression constrained to the natural historical range of 23.6–51.1 km³. The model was calibrated on official calendar-year data for 2018–2025, excluding 2017 because of a reporting inconsistency; its root mean square error (RMSE) was 1.125 km³, about 3 % of mean runoff. Missing total withdrawal values were estimated with ridge regression on year and runoff (R^2 = 0.103). These reconstructed values are treated as analytical estimates, not observations.

2.3. GIS processing

The SRTM DEM (1 arc-second, about 30 m) [23] was clipped to the study area, sinks were filled, and flow-direction and flow-accumulation rasters were derived. Cells above an accumulation threshold defined the river network; outlets and major gauging stations defined sub-basin boundaries. The derived network and boundaries were checked against HydroSHEDS [24] and corrected where they disagreed. All layers were stored in WGS 84 [25]; areas, lengths and slopes were computed in a projected coordinate system.

Annual indicators were joined to sub-basins and flow zones through shared identifiers. Basin- or sub-basin-scale values were not interpolated to finer raster cells, which avoids showing spatial detail that the data do not support. Water supply was mapped in five classes (very high, high, medium, low, very low) for 2000, 2005, 2010, 2015, 2020 and 2025, with the same class limits and colour scheme in every map so that years can be compared directly [42]. All mapping was done in ArcGIS Pro; statistics were computed in Python.

2.4. Trend, change-point and drought analysis

Linear trends were estimated by ordinary least squares. Their significance was tested with the non-parametric Mann–Kendall test [28, 29], and the magnitude with Sen's slope [30]. The Pettitt test [31] located change points. Pearson and Spearman coefficients measured association between indicators. Drought was characterised with the 12-month Standardised Precipitation Index (SPI-12) [32, 33] and Standardised Precipitation–Evapotranspiration Index (SPEI-12) [34, 35]. Because the record covers 26 years, both indices were used to rank dry and wet years within the study period, not as absolute return-period classes.

Derived indicators were computed as:

$$B_c = P - PET \qquad K_a = \frac{P}{PET} \qquad K_{wr} = \frac{W}{Q} \times 100 \qquad I_{wa} = 100 - K_{wr}$$

where B_c is the climatic water balance (mm), P annual precipitation (mm), PET potential evapotranspiration (mm), K_a the aridity ratio, W total annual withdrawal (km³), Q annual basin runoff (km³), K_wr the withdrawal-to-runoff ratio (%) and I_wa the water availability index (%). K_wr is used as a relative pressure indicator between years and scenarios, not as an absolute scarcity threshold [40, 41].

2.5. Scenario modelling to 2035

The 2000–2024 mean was taken as the climatological reference and 2025 as the current baseline. Values for 2035 under SSP1-2.6, SSP2-4.5, SSP3-7.0 and SSP5-8.5 [36] were obtained with a delta-change approach:

$$X_{2035,s} = \bar{X}_{2000\text{–}2024} \times \left(1 + \frac{\Delta_s}{100}\right)$$

where Δ_s is the percentage change for scenario s; temperature changes were added in °C. Change ranges (Table 2) were aligned with CMIP6-based regional projections and downscaled datasets for Central Asia [36–38].

Scenario	Temperature, °C	Precipitation, %	PET, %	Snowfall, %
SSP1-2.6	+0.55 to +0.95	−3 to +5	+2 to +6	−12 to −4
SSP2-4.5	+0.65 to +1.15	−5 to +5	+3 to +7	−15 to −5
SSP3-7.0	+0.75 to +1.35	−7 to +5	+4 to +9	−19 to −7
SSP5-8.5	+0.85 to +1.55	−9 to +5	+5 to +11	−23 to −9

Table 2. Change ranges applied for 2035 relative to 2000–2024.

The 2035 meteorological values were entered into the calibrated regression to obtain runoff, and results were checked against historical extremes and published regional ranges. Withdrawal was projected with the ridge model as an auxiliary indicator. Results are reported as median values with lower and upper bounds. Uncertainty from data, model structure and scenario choice is described following IPCC guidance [39].

3. RESULTS

3.1. Climate trends, 2000–2024

Temperature and PET increased significantly, while precipitation and the climatic water balance showed no significant trend (Table 3). Mean annual temperature rose by 0.0329 °C yr^{-1} (Sen's slope 0.032 °C yr^{-1}). The Pettitt test placed a change point in 2013 (p = 0.012): mean temperature was 9.72 °C in 2000–2012 and 10.19 °C in 2013–2024. Years above 10.3 °C (2014, 2015, 2019, 2020, 2023 and 2024) all fall after the change point, and 2024 was the warmest year (10.51 °C).

Indicator	Mean 2000–2024	Minimum (year)	Maximum (year)	Linear trend per year	Kendall τ	p
Air temperature, °C	9.94	9.10 (2003)	10.51 (2024)	+0.0329	0.427	0.003
Precipitation, mm	317.65	233.30 (2007)	428.05 (2009)	−0.31	–	n.s.
PET, mm	1044.01	1011.19 (2003)	1065.40 (2020)	+1.198	0.367	0.011
Climatic water balance, mm	−726.36	−809.07 (2007)	−606.07 (2009)	−1.50	–	n.s.
Toktogul inflow, km^3	13.37	9.91 (2007)	19.20 (2009)	−0.021	–	n.s.
Basin runoff, km^3	37.95	27.64 (2007)	50.29 (2009)	−0.068	−0.080	0.591
Withdrawal-to-runoff ratio, %	35.73	27.08 (2009)	47.40 (2007)	–	0.093	0.528

Table 3. Descriptive statistics and trends of hydroclimatic indicators, 2000–2024 (n.s. = not significant at p < 0.05).

Precipitation varied strongly from year to year (coefficient of variation 13.17 %). The 195 mm gap between 2007 and 2009 equals more than 61 % of the mean, while the difference between the two sub-periods was only 1.74 mm (316.81 vs 318.55 mm). PET, by contrast, rose steadily, by 16.79 mm (1.62 %) from 2000–2012 to 2013–2024, with a change point also

near 2013. The climatic water balance was negative in every year (Fig. 2).

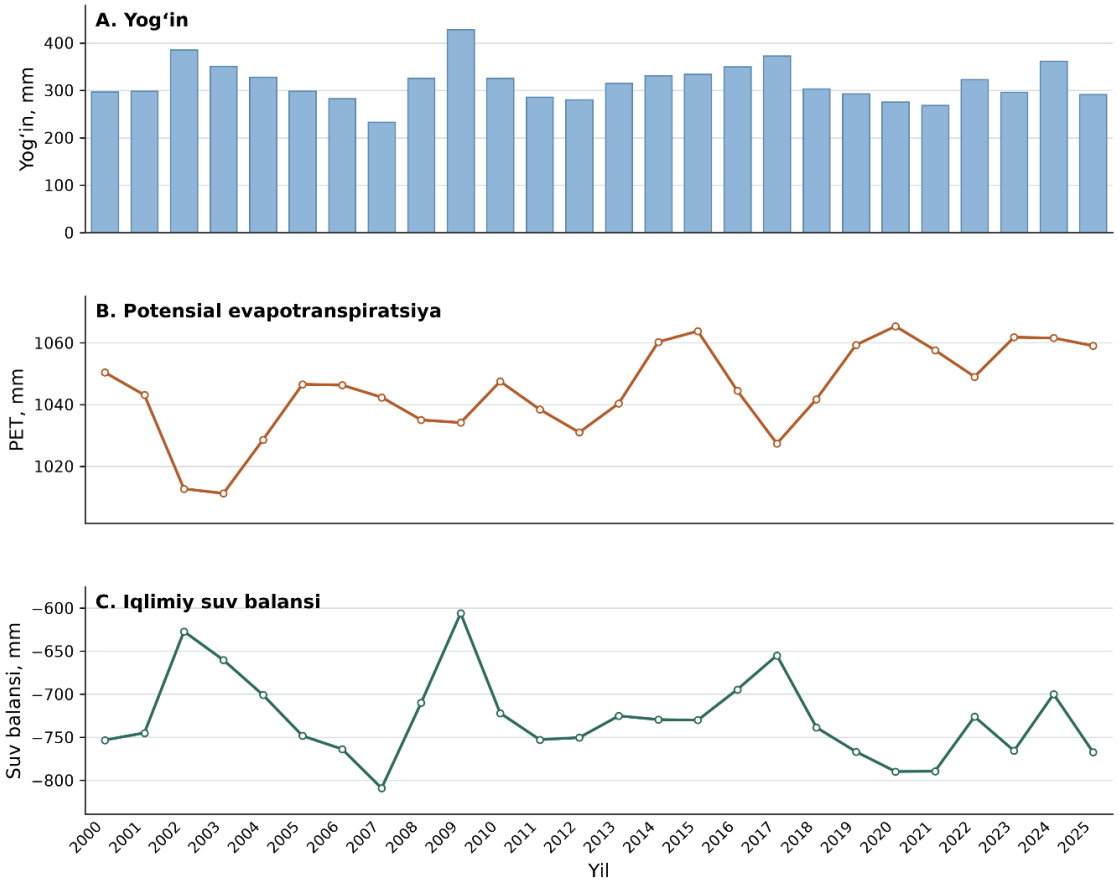


Fig. 2. Annual precipitation, PET and climatic water balance, 2000–2025.

SPI-12 and SPEI-12 identified 2007 as the driest year (−2.63 and −4.29) and 2009 as the wettest (SPI-12 = 2.92). Two consecutive dry years occurred in 2020 and 2021 (SPI-12 = −1.22 and −1.45). After a wet 2024 (SPI-12 = 1.26), the index fell again to −0.72 in 2025. Neither index showed a long-term trend, so the main hazard is the alternation of very dry and very wet years rather than a steady decline (Fig. 3).

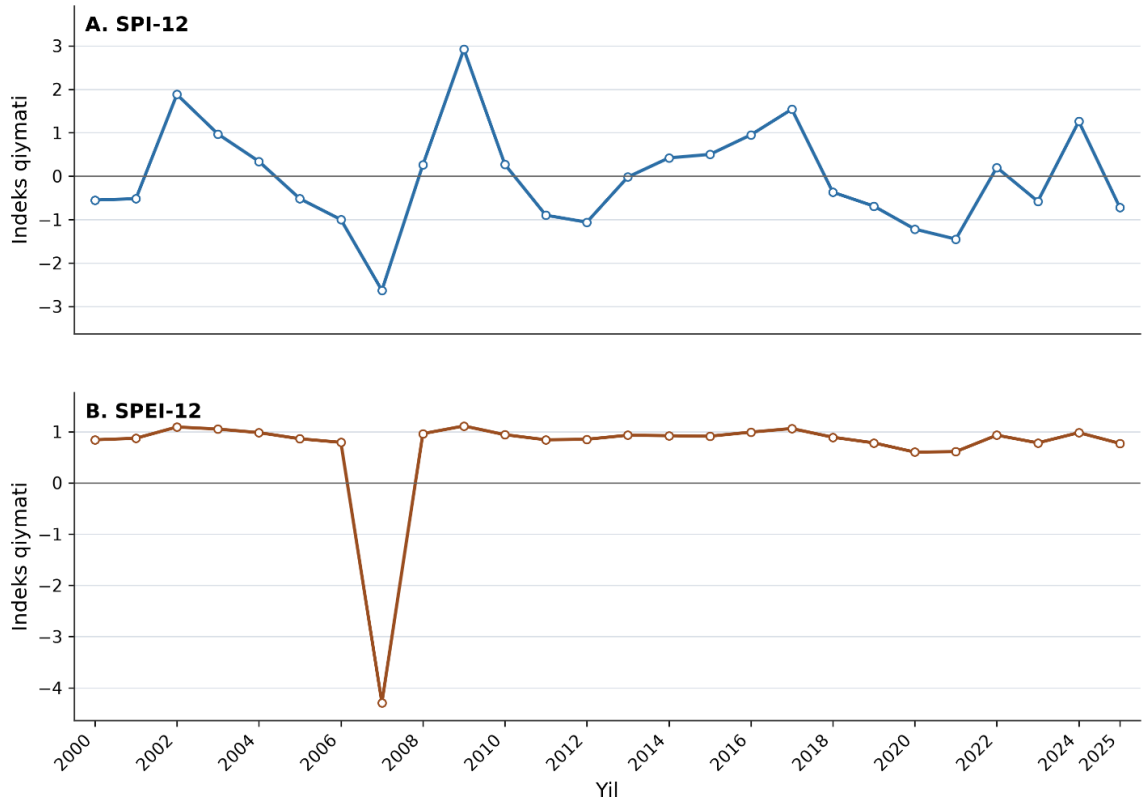


Fig. 3. SPI-12 and SPEI-12, 2000–2025.

3.2. Toktogul inflow, basin runoff and withdrawal

Toktogul inflow and basin runoff moved almost in parallel (Pearson r = 0.946, Spearman ρ = 0.988), reaching their minimum in 2007 and maximum in 2009 (Fig. 4). Runoff declined after 2019 to 32.24 km³ in 2020 and 32.09 km³ in 2021, recovered to 39.73 km³ in 2022, fell to 35.28 km³ in 2023, rose to 41.99 km³ in 2024 and dropped again to 33.25 km³ in 2025. The 8.74 km³ fall between 2024 and 2025 illustrates the basin's high interannual variability. Mean runoff barely changed between 2000–2012 (38.06 km³) and 2013–2024 (37.83 km³).

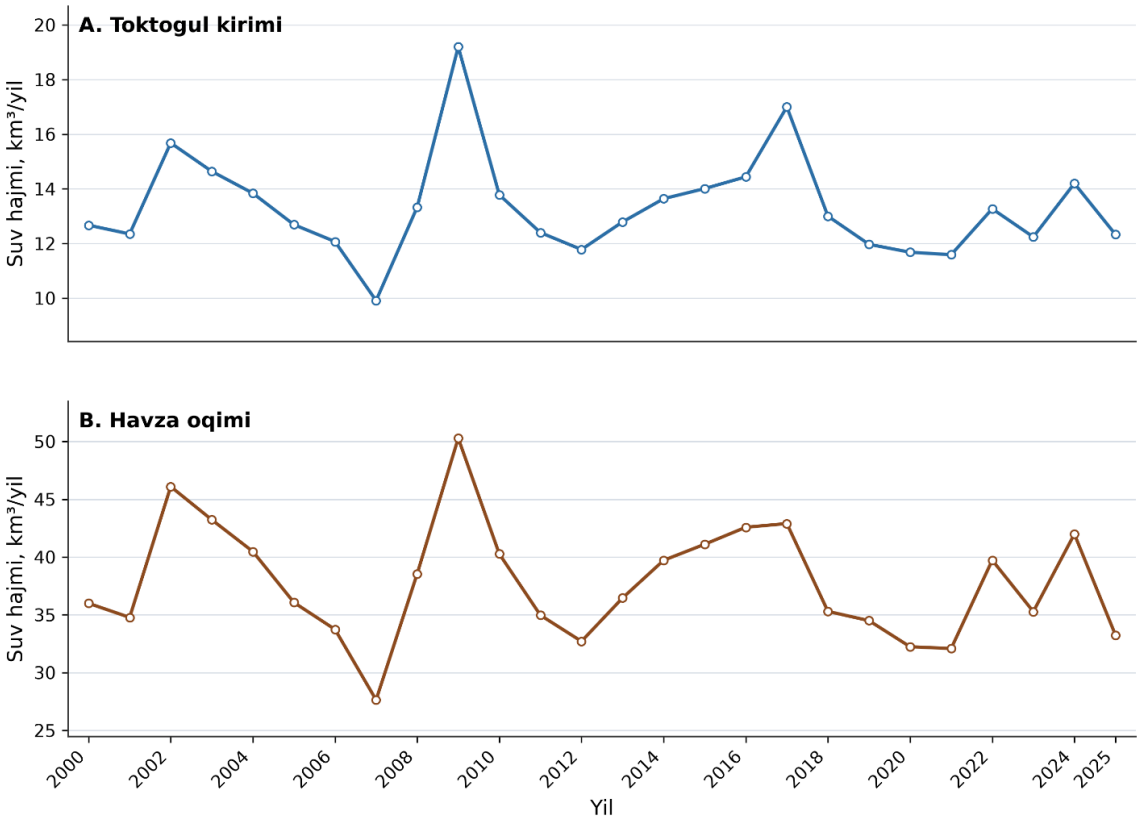


Fig. 4. Toktogul inflow and annual basin runoff, 2000–2025.

Runoff correlated strongly with precipitation (r = 0.984), SPI-12 (r = 0.986) and the climatic water balance (r = 0.950), and moderately and inversely with PET (r = −0.397, p = 0.049). Part of these very high coefficients reflects the harmonisation and reconstruction of the series (Section 2.2), so they are read as indicators of hydroclimatic consistency, not as proof of causality.

Total withdrawal averaged 13.35 km³ and stayed within 12.00–14.10 km³, so the withdrawal-to-runoff ratio was governed mainly by natural supply. In dry 2007, withdrawal of about 13.10 km³ equalled 47.40 % of runoff; in wet 2009, a larger withdrawal of 13.62 km³ equalled only 27.08 %.

3.3. Spatio-temporal pattern of water supply

Water supply fell consistently from the mountain runoff-formation zone towards the middle and lower reaches in all six mapped years (Figs. 5 and 6; Table 4). The upper zone remained in the high and very high classes throughout. The middle zone was the most variable, and the lower reaches were the most exposed, staying in the low and very low classes even in wet years.

Year	Temperature, °C	Precipitation, mm	PET, mm	Climatic water balance, mm	Toktogul inflow, km³	Basin runoff, km³	Withdrawal, km³	Withdrawal/runoff, %
2025	10.39	291.65	1059.06	−767.41	12.33	33.25	13.33	40.09
2020	10.49	275.59	1065.40	−789.80	11.68	32.24	12.41	38.49
2015	10.47	333.70	1063.81	−730.11	14.01	41.11	13.44	32.69
2010	10.03	325.55	1047.50	−721.95	13.78	40.27	13.40	33.27

Year	Temperature, °C	Precipitation, mm	PET, mm	Climatic water balance, mm	Toktogul inflow, km³	Basin runoff, km³	Withdrawal, km³	Withdrawal/runoff, %
2005	9.99	298.22	1046.59	−748.37	12.69	36.07	13.28	36.82
2000	10.09	297.18	1050.41	−753.23	12.67	36.00	13.26	36.83

Table 4. Basin indicators for the six mapped years.

The 2000 and 2005 maps are almost identical, as their runoff differed by only 0.07 km³. In 2010 and 2015, higher runoff (40.27 and 41.11 km³) at similar withdrawal moved parts of the Fergana Valley and middle reaches from the low to the medium class. In 2015 this happened despite high temperature and PET, showing that ample runoff can offset higher atmospheric demand. In 2020, low precipitation, the highest PET of the record and low runoff pushed the low and very low classes upstream from the lower into the middle reaches. In 2025 runoff was 1.01 km³ higher than in 2020, but withdrawal was 0.92 km³ higher as well, so the stressed zones in the middle and lower reaches did not shrink.

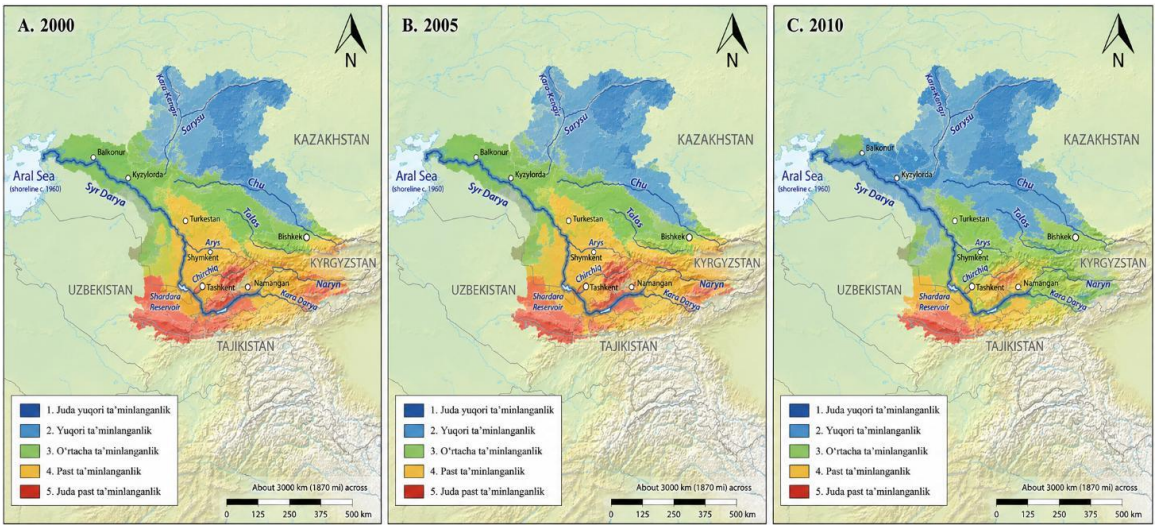


Fig. 5. Water supply classes in 2000, 2005 and 2010.

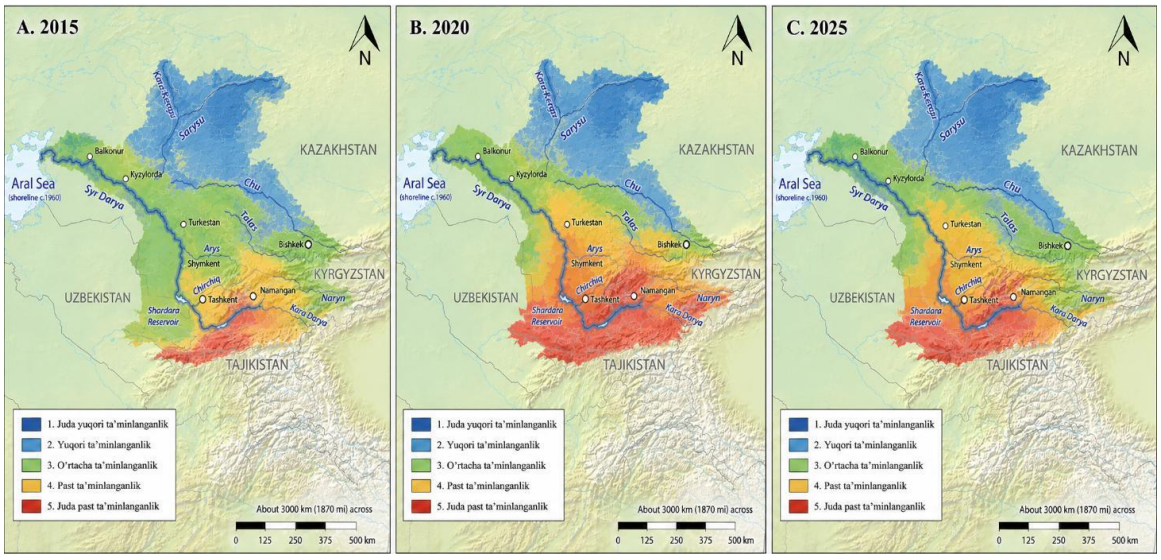


Fig. 6. Water supply classes in 2015, 2020 and 2025.

3.4. The 2025 baseline

2025 was not an extreme drought year, but it was drier than normal and under higher water-use pressure (Table 5; Fig. 7). Temperature and PET were above the mean; precipitation, snowfall, Toktogul inflow and runoff were below it. Because withdrawal stayed at the long-term level, the withdrawal-to-runoff ratio rose by 4.36 percentage points to 40.09 %. Toktogul released 1.64 km³ more than it received, drawing on storage accumulated in earlier years.

Indicator	Unit	Mean 2000–2024	2025	Difference, %
Air temperature	°C	9.94	10.39	+4.46
Precipitation	mm	317.65	291.65	−8.18
Snowfall	mm	110.37	93.20	−15.56
Maximum snow water equivalent	mm	–	84.81	−6.85
PET	mm	1044.01	1059.06	+1.44
Climatic water balance	mm	−726.36	−767.41	−5.65
Aridity ratio (P/PET)	–	0.305	0.275	−9.57
Toktogul inflow	km³	13.37	12.33	−7.76
Toktogul outflow	km³	13.71	13.97	+1.91
Basin runoff	km³	37.95	33.25	−12.38
Total withdrawal	km³	13.35	13.33	−0.18
Withdrawal-to-runoff ratio	%	35.73	40.09	+12.21
Water availability index	%	64.27	59.91	−6.79

Table 5. The 2025 baseline compared with the 2000–2024 mean.

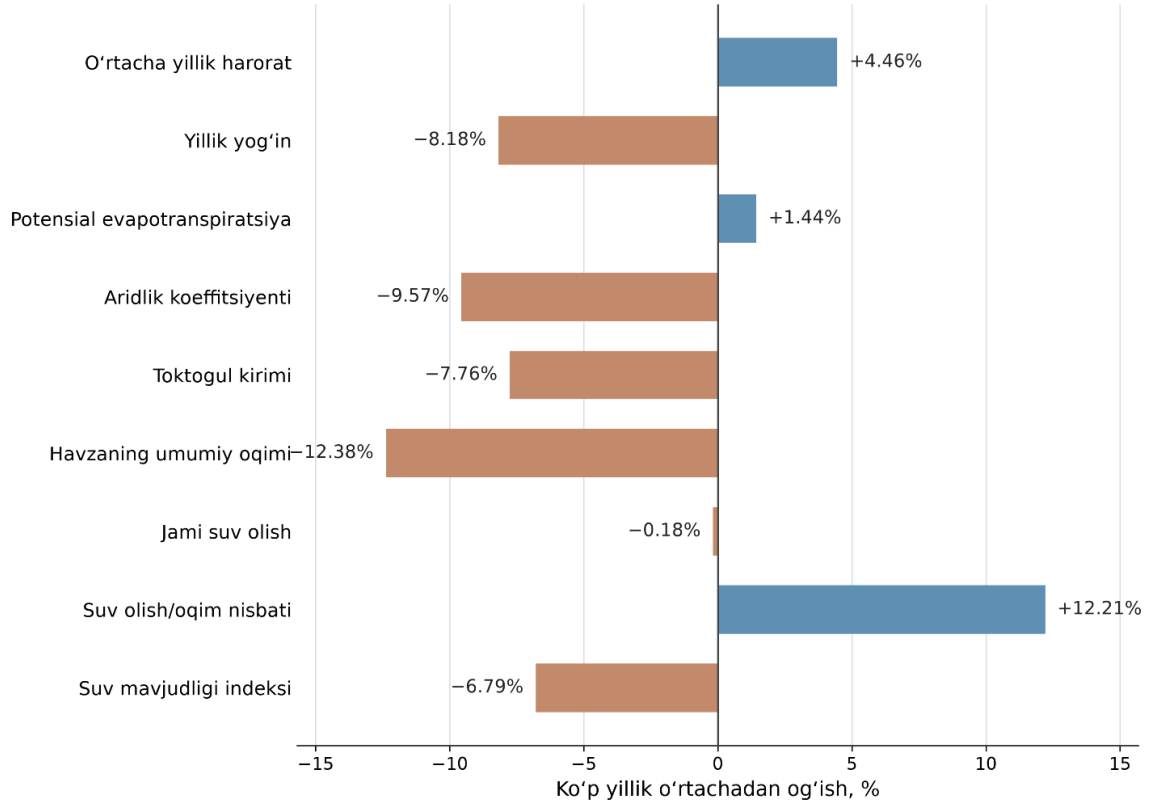


Fig. 7. Deviation of 2025 indicators from the 2000–2024 mean.

3.5. Meteorological change to 2035

All four scenarios point to a hotter and more arid basin by 2035, driven by rising PET rather than falling precipitation (Table 6; Fig. 8). Median temperature rises from 9.94 °C to 10.69–11.14 °C, while precipitation changes by only +1 % to −2 %. PET increases by 4–7 %, so the climatic water balance deteriorates by 38.58–79.43 mm and snowfall declines by 8–16 %.

Indicator	Reference 2000–2024	SSP1-2.6	SSP2-4.5	SSP3-7.0	SSP5-8.5
Air temperature, °C	9.94	10.69	10.84	10.99	11.14
Precipitation, mm	317.65	320.82	317.65	314.47	311.29
PET, mm	1044.01	1085.77	1096.21	1106.65	1117.09
Climatic water balance, mm	−726.36	−764.94	−778.56	−792.18	−805.79
Aridity ratio	0.304	0.295	0.290	0.284	0.279
Snowfall, mm	110.37	101.54	99.33	96.02	92.71

Table 6. Median meteorological projections for 2035.

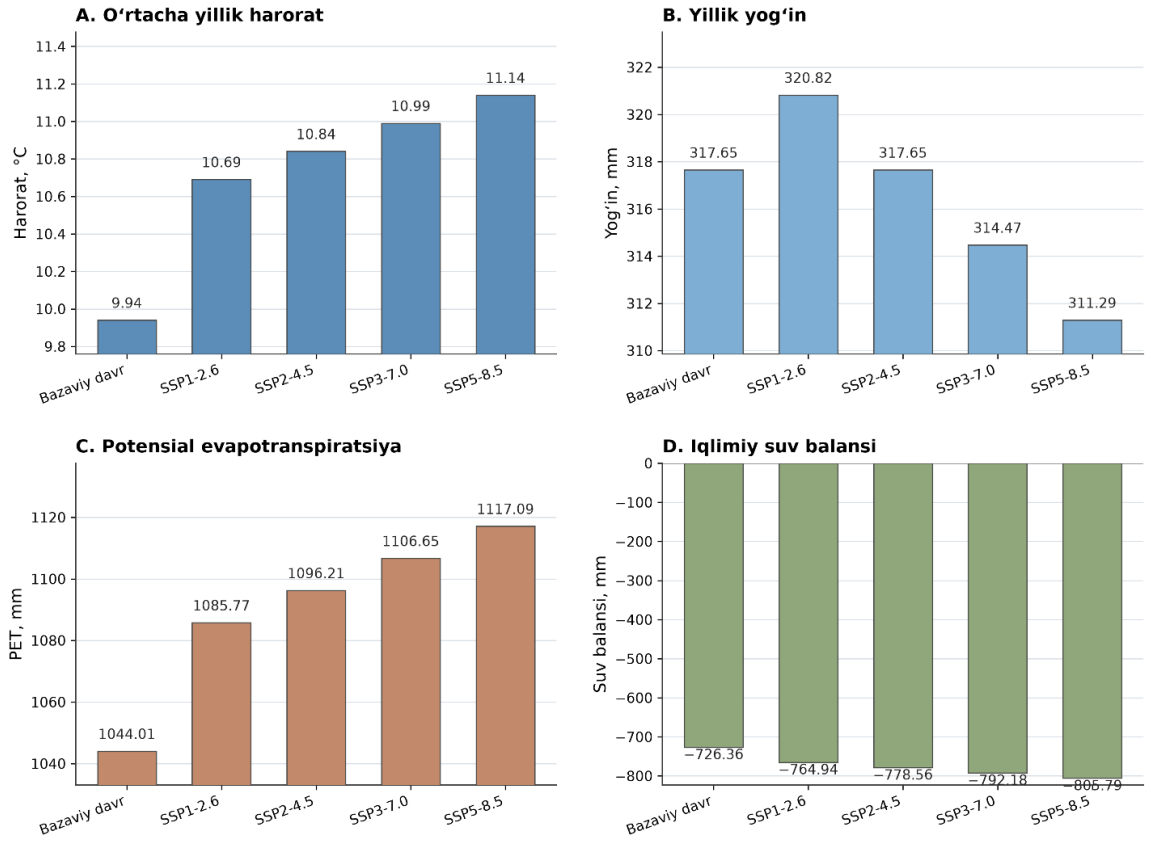


Fig. 8. Main meteorological indicators in 2035 by scenario.

Warming is strongest in winter: +0.86 °C under SSP1-2.6 and +1.38 °C under SSP5-8.5, against +0.69 °C and +1.10 °C in summer. The summer water deficit worsens most. Under SSP5-8.5, summer precipitation falls by 7 % (45.43 to 42.25 mm) while summer PET rises by 8.05 % (507.79 to 548.67 mm), bringing the summer climatic water balance to −506.42 mm; the spring balance falls to −194.70 mm (Fig. 9). Uncertainty is larger for precipitation than for temperature: under SSP5-8.5 the plausible range is 10.79–11.49 °C for temperature but 289.06–333.53 mm for precipitation.

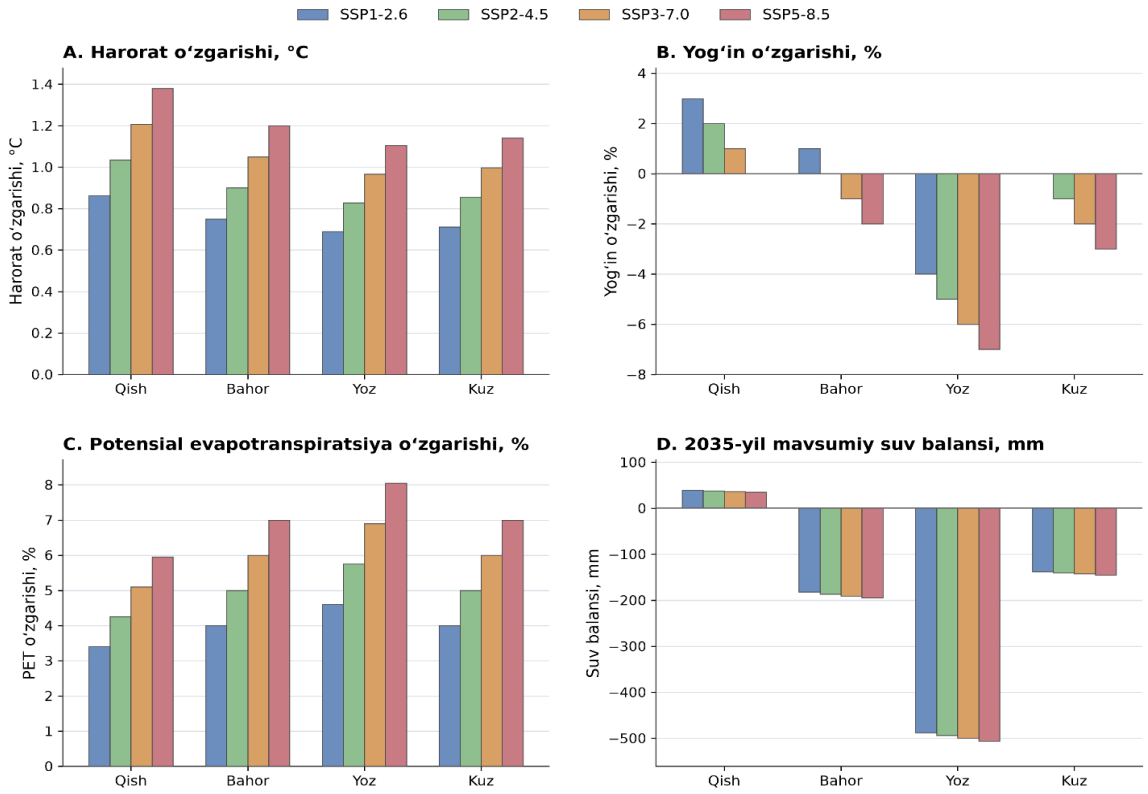


Fig. 9. Seasonal change in meteorological indicators by 2035.

3.6. Runoff, withdrawal and water stress to 2035

Basin runoff in 2035 is projected at 37.85 km³ under SSP1-2.6, falling to 36.48 km³ under SSP5-8.5, i.e. 0.25–3.87 % below the 2000–2024 mean (Table 7). All values exceed the dry 2025 baseline by 9.71–13.84 %, but none returns to the long-term mean. Withdrawal rises slowly to 13.50–13.59 km³, so the withdrawal-to-runoff ratio climbs from 35.67 % to 37.26 % across the scenarios, and the residual flow after withdrawal shrinks from 24.35 to 22.89 km³.

Indicator	Mean 2000–2024	2025	SSP1-2.6	SSP2-4.5	SSP3-7.0	SSP5-8.5
Basin runoff, km³	37.95	33.25	37.85	37.45	36.97	36.48
Change vs 2000–2024 mean, %	–	−12.38	−0.25	−1.31	−2.59	−3.87
Total withdrawal, km³	13.35	13.33	13.50	13.53	13.56	13.59
Withdrawal-to-runoff ratio, %	35.73	40.09	35.67	36.14	36.69	37.26
Water availability index, %	64.27	59.91	64.33	63.86	63.31	62.74
Residual flow after withdrawal, km³	–	19.92	24.35	23.92	23.40	22.89

Table 7. Runoff and water-stress indicators for 2035 (median values).

The spread between SSP1-2.6 and SSP5-8.5 (1.37 km³, 3.62 % of mean runoff) is close to the reconstruction model's RMSE (1.125 km³, 2.96 %). The 0.25 % decline under SSP1-2.6 therefore cannot be distinguished from zero, whereas the declines under SSP3-7.0 and SSP5-8.5 are supported by the consistent direction of all meteorological drivers. At basin scale, each 1 % of runoff equals about 0.38 km³.

Exposure differs sharply between zones (Table 8; Figs. 10 and 11). Under SSP5-8.5, low and very low supply classes may extend from the lower into the middle reaches.

Zone	Main water source	Main pressure	2025	2035, SSP2-4.5	2035, SSP5-8.5
Upper	Snow, glacier and mountain-river runoff	Less snowfall, earlier melt	Relatively favourable	Medium risk	Medium-high risk
Middle	Reservoir-regulated flow	Irrigation demand, rising PET	Medium pressure	Medium pressure	High pressure
Lower	Inflow from upstream	Cumulative withdrawal, evaporation, lower runoff	High risk	High risk	Very high risk

Table 8. Sensitivity of basin zones to water stress.

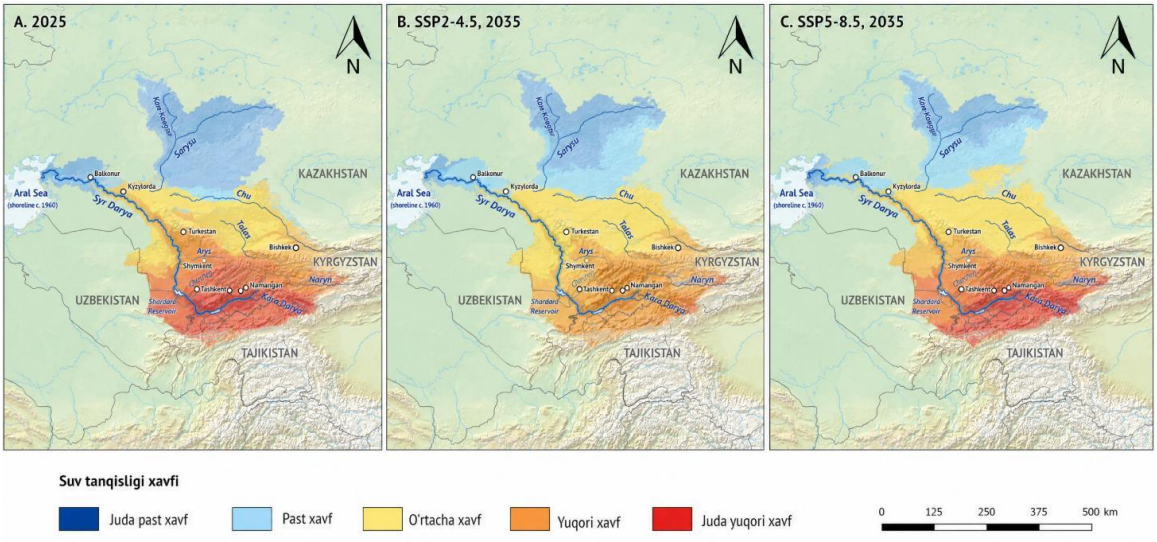


Fig. 10. Water-stress risk in 2025 and in 2035 under SSP2-4.5 and SSP5-8.5.

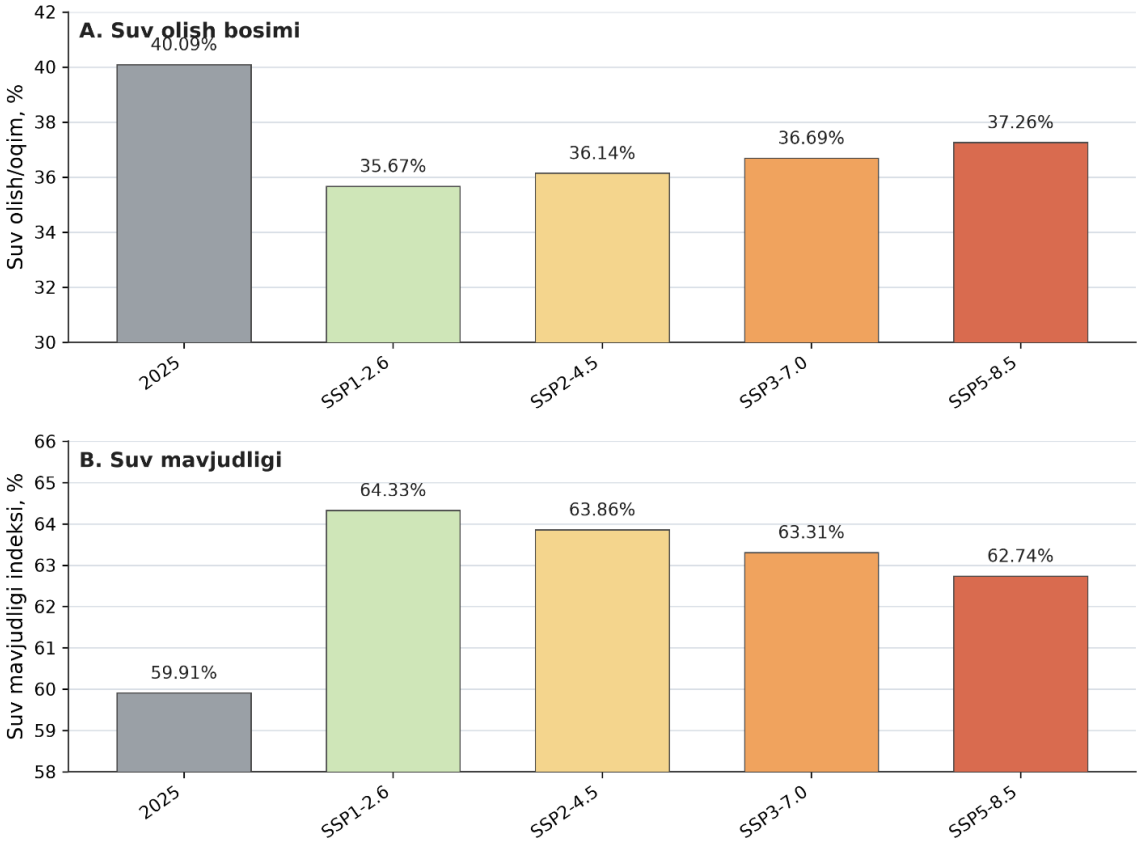


Fig. 11. Withdrawal-to-runoff ratio and water availability index in 2025 and 2035.

4. DISCUSSION

4.1. Warming without drying

The central finding is that the Syr Darya basin is warming and its atmospheric water demand is rising, while precipitation and runoff show no significant trend. Temperature rose by 0.0329 °C yr^{-1} with a shift around 2013, and PET rose by 1.198 mm yr^{-1}; precipitation and runoff varied widely but did not decline. This pattern agrees with the expectation that warming first changes the timing and partitioning of water in snow-dominated basins before it changes annual totals [1, 2]. It also agrees with work showing glacier shrinkage in the Tien Shan [4] and a declining snowfall fraction in Central Asian alpine zones [6]: snowfall in 2025 was 15.56 % below the mean, and all scenarios project a further 8–16 % decline by 2035.

The absence of a runoff trend should not be read as stability. Glacier melt can sustain or even raise runoff for some decades before it declines [2], and part of the present flow may come from this temporary source. Studies of the basin's runoff have found that both climatic and human factors shape its long-term behaviour [11–13], and our results support this. Runoff tracks precipitation and upstream inflow closely, while withdrawal stays almost constant, so stress rises sharply in dry years.

4.2. Pressure comes from supply variability, not rising demand

Total withdrawal changed little over 26 years (12.00–14.10 km^3), yet the withdrawal-to-runoff ratio ranged from 27.08 % to 47.40 %. Water stress in the basin is therefore driven mainly by variability in natural supply acting on a rigid demand. In 2025, a 12.38 % runoff deficit with unchanged withdrawal raised the ratio to 40.09 %. The same mechanism appears in the projections: the scenario runoff decline is modest (0.25–3.87 %), but slowly rising withdrawal narrows the margin, and the residual flow falls by 1.46 km^3 between SSP1-2.6 and SSP5-8.5.

The projected decline is consistent in direction with model-based studies of Central Asian catchments and the upper Syr Darya [14–17]. The strongest signal is seasonal: higher winter temperatures, less snowfall and a summer climatic water balance of −506.42 mm under SSP5-8.5 point to earlier runoff and drier summers. Similar shifts in discharge timing and soil moisture have been projected for the Naryn catchment [16].

4.3. Spatial asymmetry and transboundary implications

The maps show a persistent gradient from well-supplied mountains to stressed lowlands. This mirrors the geography of the basin: water forms mainly upstream and is used mainly downstream. Analyses of transboundary basins show that upstream water use is a major cause of downstream stress [41], and the lower Syr Darya fits this pattern. Its supply depends on what remains after cumulative withdrawals, reservoir operation and evaporation upstream. When runoff falls, the low-supply zone does not stay in place but extends into the middle reaches, as in 2020.

These results have three practical implications. First, planning based on annual totals underestimates risk, because the critical deficit occurs in the summer irrigation season. Second, the conflict between winter hydropower releases and summer irrigation demand at Toktogul [10] will matter more as snow storage declines and the seasonal role of reservoirs grows. Third, adaptation should give priority to the lower reaches and to measures that reduce rigid demand: water-saving irrigation, canal lining and seasonal allocation rules that respond to forecast inflow [17, 43].

4.4. Limitations

Several limitations define how the results should be used.

- **Harmonised and reconstructed data.** Climate and snow series are basin-scale harmonised series, not direct station or satellite values; parts of the runoff and withdrawal records were reconstructed (RMSE 1.125 km³; withdrawal R^2 = 0.103). Correlations are therefore partly inflated by the method.
- **Annual, basin-scale projections.** Runoff and withdrawal were projected for the whole basin and per year. Sub-basin, gauging-station and monthly projections were not produced, and zone sensitivity (Table 8) is qualitative.
- **Delta-change approach.** Delta scaling preserves the reference variability and does not represent changes in extremes or in the sequence of dry and wet years.
- **Processes not modelled.** Return flows, groundwater exchange, water quality, environmental flow requirements and future reservoir operating rules were not included.

Future work should move to monthly time steps, use bias-adjusted CMIP6 ensembles at sub-basin scale [37, 38], and add satellite-based mapping of irrigated area and terrestrial water storage [44–46].

5. CONCLUSIONS

This study combined climate, snow, reservoir, runoff and withdrawal data for the whole Syr Darya basin in one statistical and GIS framework for 2000–2025 and extended it to 2035 under four SSP scenarios. The main conclusions are:

1. Air temperature (+0.0329 °C yr^{-1}, change point in 2013) and PET (+1.198 mm yr^{-1}) increased significantly, whereas precipitation and runoff showed no significant trend but strong interannual variability (runoff 27.64–50.29 km³).
2. Water stress is driven mainly by variability in natural supply acting on near-constant withdrawal (about 13.35 km³); the withdrawal-to-runoff ratio ranged from 27.08 % in a wet year to 47.40 % in a dry year.
3. In the 2025 baseline, runoff was 33.25 km³ (−12.38 %), the withdrawal-to-runoff ratio rose to 40.09 % and the water availability index fell to 59.91 %.
4. Water supply declines consistently from the upper to the lower basin; in dry years the low-supply zone expands from the lower into the middle reaches.
5. By 2035, runoff is projected at 36.48–37.85 km³ (0.25–3.87 % below the 2000–2024 mean), snowfall falls by 8–16 %, and the summer climatic water balance reaches −506.42 mm under SSP5-8.5. The lower reaches and the summer irrigation season are the most exposed.

Water management in the basin should therefore plan for seasonal and spatial deficits, not only annual totals, and give priority to demand flexibility in the middle and lower reaches.

Declarations

Author contributions. A.O. Hasanov: conceptualisation, data curation, formal analysis, GIS mapping, writing – original draft. B.A. Pulatov: supervision, methodology, writing – review and editing. *(Confirm before submission.)*

Funding. [To be added, or "This research received no external funding."]

Data availability. The harmonised dataset and GIS layers are available from the corresponding author on reasonable request.

Conflict of interest. The authors declare no conflict of interest.

Acknowledgements. The results were implemented with the support of the Main Departments of Ecology and Climate Change of Andijan, Namangan and Syrdarya regions and the National Committee for Ecology and Climate Change of the Republic of Uzbekistan.

REFERENCES

1. Barnett, T.P., Adam, J.C., Lettenmaier, D.P. (2005). Potential impacts of a warming climate on water availability in snow-dominated regions. *Nature*, 438(7066), 303–309. https://doi.org/10.1038/nature04141
2. Huss, M., Hock, R. (2018). Global-scale hydrological response to future glacier mass loss. *Nature Climate Change*, 8(2), 135–140. https://doi.org/10.1038/s41558-017-0049-x
3. Immerzeel, W.W., Lutz, A.F., Andrade, M., et al. (2020). Importance and vulnerability of the world's water towers. *Nature*, 577(7790), 364–369. https://doi.org/10.1038/s41586-019-1822-y
4. Sorg, A., Bolch, T., Stoffel, M., Solomina, O., Beniston, M. (2012). Climate change impacts on glaciers and runoff in Tien Shan (Central Asia). *Nature Climate Change*, 2(10), 725–731. https://doi.org/10.1038/nclimate1592
5. Chen, Y., Li, W., Deng, H., Fang, G., Li, Z. (2016). Changes in Central Asia's water tower: past, present and future. *Scientific Reports*, 6, 35458. https://doi.org/10.1038/srep35458
6. Li, Z., Chen, Y., Li, Y., et al. (2020). Declining snowfall fraction in the alpine regions, Central Asia. *Scientific Reports*, 10, 3476. https://doi.org/10.1038/s41598-020-60303-z
7. Sorg, A., Mosello, B., Shalpykova, G., Allan, A., Hill Clarvis, M., Stoffel, M. (2014). Coping with changing water resources: the case of the Syr Darya river basin in Central Asia. *Environmental Science & Policy*, 43, 68–77. https://doi.org/10.1016/j.envsci.2013.11.003
8. UNECE (2011). *Second Assessment of Transboundary Rivers, Lakes and Groundwaters*. United Nations, New York and Geneva.
9. Rakhmatullaev, S., Huneau, F., Le Coustumer, P., Motelica-Heino, M., Bakiev, M. (2010). Facts and perspectives of water reservoirs in Central Asia: a special focus on Uzbekistan. *Water*, 2(2), 307–320. https://doi.org/10.3390/w2020307
10. Bernauer, T., Siegfried, T. (2012). Climate change and international water conflict in Central Asia. *Journal of Peace Research*, 49(1), 227–239. https://doi.org/10.1177/0022343311425843
11. Zou, S., Abuduwaili, J., Duan, W., De Maeyer, P., Van de Voorde, T. (2019). Human and natural impacts on the water resources in the Syr Darya River Basin, Central Asia. *Sustainability*, 11(11), 3084. https://doi.org/10.3390/su11113084
12. Bissenbayeva, S., Abuduwaili, J., Saparova, A., Ahmed, T. (2021). Long-term variations in runoff of the Syr Darya River Basin under climate change and human activities. *Journal of Arid Land*, 13(1), 56–70. https://doi.org/10.1007/s40333-021-0050-0
13. Zhai, X.B., Li, Y.P., Liu, Y.R., Huang, G.H. (2021). Assessment of the effects of human activity and natural condition on the outflow of Syr Darya River: a stepwise-cluster factorial analysis method. *Environmental Research*, 194, 110634. https://doi.org/10.1016/j.envres.2020.110634
14. Didovets, I., Lobanova, A., Krysanova, V., et al. (2021). Central Asian rivers under climate change: impacts assessment in eight representative catchments. *Journal of Hydrology: Regional Studies*, 34, 100779. https://doi.org/10.1016/j.ejrh.2021.100779
15. Kalashnikova, O.Yu., Niyazov, J., Nurbatsina, A., Kodirov, S., Radchenko, Y., Kretova, Z. (2023). Kyrgyz transboundary rivers' runoff assessment: Syr-Darya and Amu-Darya river basins in climate change scenarios. *Central Asian Journal of Water Research*, 9(1), 59–88.
16. Schaffhauser, T., Lange, S., Tuo, Y., Disse, M. (2023). Shifted discharge and drier soils: hydrological projections for a Central Asian catchment. *Journal of Hydrology: Regional Studies*, 46, 101338. https://doi.org/10.1016/j.ejrh.2023.101338
17. Zhai, X.B., Li, Y.P., Wang, H., Huang, G.H., Li, Y. (2023). Assessment of the potential impacts of climate changes on Syr Darya watershed: a hybrid ensemble analysis method. *Journal of Hydrology: Regional Studies*, 47, 101415. https://doi.org/10.1016/j.ejrh.2023.101415
18. SIC ICWC. *Water resources of the Syr Darya River basin* [online]. Scientific-Information Center of the

Interstate Commission for Water Coordination of Central Asia, Tashkent. Accessed 4 August 2026.

19. SIC ICWC. *Water management infrastructure of the Syr Darya River basin* [online]. Tashkent. Accessed 4 August 2026.
20. Muñoz-Sabater, J., Dutra, E., Agustí-Panareda, A., et al. (2021). ERA5-Land: a state-of-the-art global reanalysis dataset for land applications. *Earth System Science Data*, 13(9), 4349–4383. https://doi.org/10.5194/essd-13-4349-2021
21. Harris, I., Osborn, T.J., Jones, P., Lister, D. (2020). Version 4 of the CRU TS monthly high-resolution gridded multivariate climate dataset. *Scientific Data*, 7, 109. https://doi.org/10.1038/s41597-020-0453-3
22. Hall, D.K., Riggs, G.A., Salomonson, V.V., DiGirolamo, N.E., Bayr, K.J. (2002). MODIS snow-cover products. *Remote Sensing of Environment*, 83(1–2), 181–194. https://doi.org/10.1016/S0034-4257(02)00095-0
23. Farr, T.G., Rosen, P.A., Caro, E., et al. (2007). The Shuttle Radar Topography Mission. *Reviews of Geophysics*, 45(2), RG2004. https://doi.org/10.1029/2005RG000183
24. Lehner, B., Verdin, K., Jarvis, A. (2008). New global hydrography derived from spaceborne elevation data. *Eos, Transactions AGU*, 89(10), 93–94. https://doi.org/10.1029/2008EO100001
25. NGA (2014). *Department of Defense World Geodetic System 1984: Its Definition and Relationships with Local Geodetic Systems*. NGA.STND.0036_1.0.0_WGS84. National Geospatial-Intelligence Agency, Springfield, VA.
26. WMO (2020). *Guide to Hydrological Practices, Volume I*. WMO-No. 168. World Meteorological Organization, Geneva.
27. Wilkinson, M.D., Dumontier, M., Aalbersberg, I.J., et al. (2016). The FAIR Guiding Principles for scientific data management and stewardship. *Scientific Data*, 3, 160018. https://doi.org/10.1038/sdata.2016.18
28. Mann, H.B. (1945). Nonparametric tests against trend. *Econometrica*, 13(3), 245–259. https://doi.org/10.2307/1907187
29. Kendall, M.G. (1975). *Rank Correlation Methods*, 4th ed. Charles Griffin, London.
30. Sen, P.K. (1968). Estimates of the regression coefficient based on Kendall's tau. *Journal of the American Statistical Association*, 63(324), 1379–1389. https://doi.org/10.1080/01621459.1968.10480934
31. Pettitt, A.N. (1979). A non-parametric approach to the change-point problem. *Journal of the Royal Statistical Society, Series C*, 28(2), 126–135. https://doi.org/10.2307/2346729
32. McKee, T.B., Doesken, N.J., Kleist, J. (1993). The relationship of drought frequency and duration to time scales. In: *Proceedings of the 8th Conference on Applied Climatology*, Anaheim, CA, 179–184.
33. WMO (2012). *Standardized Precipitation Index User Guide* (Svoboda, M., Hayes, M., Wood, D.). WMO-No. 1090. Geneva.
34. Vicente-Serrano, S.M., Beguería, S., López-Moreno, J.I. (2010). A multiscalar drought index sensitive to global warming: the Standardized Precipitation Evapotranspiration Index. *Journal of Climate*, 23(7), 1696–1718. https://doi.org/10.1175/2009JCLI2909.1
35. Beguería, S., Vicente-Serrano, S.M., Reig, F., Latorre, B. (2014). Standardized precipitation evapotranspiration index (SPEI) revisited: parameter fitting, evapotranspiration models, tools, datasets and drought monitoring. *International Journal of Climatology*, 34(10), 3001–3023. https://doi.org/10.1002/joc.3887
36. IPCC (2021). *Climate Change 2021: The Physical Science Basis*. Contribution of Working Group I to the Sixth Assessment Report. Cambridge University Press. https://doi.org/10.1017/9781009157896
37. Thrasher, B., Wang, W., Michaelis, A., Melton, F., Lee, T., Nemani, R. (2022). NASA Global Daily Downscaled Projections, CMIP6. *Scientific Data*, 9, 262. https://doi.org/10.1038/s41597-022-01393-4
38. Lange, S. (2019). Trend-preserving bias adjustment and statistical downscaling with ISIMIP3BASD (v1.0). *Geoscientific Model Development*, 12(7), 3055–3070. https://doi.org/10.5194/gmd-12-3055-2019
39. Mastrandrea, M.D., Field, C.B., Stocker, T.F., et al. (2010). *Guidance Note for Lead Authors of the IPCC Fifth Assessment Report on Consistent Treatment of Uncertainties*. IPCC, Geneva.

40. Kummu, M., Guillaume, J.H.A., de Moel, H., et al. (2016). The world's road to water scarcity: shortage and stress in the 20th century and pathways towards sustainability. *Scientific Reports*, 6, 38495. https://doi.org/10.1038/srep38495

41. Munia, H., Guillaume, J.H.A., Mirumachi, N., Porkka, M., Wada, Y., Kummu, M. (2016). Water stress in global transboundary river basins: significance of upstream water use on downstream stress. *Environmental Research Letters*, 11(1), 014002. https://doi.org/10.1088/1748-9326/11/1/014002

42. Brewer, C.A. (2015). *Designing Better Maps: A Guide for GIS Users*, 2nd ed. Esri Press, Redlands, CA.

43. Huang, J., Bashiri, Z., Disse, M. (2026). Climate-informed water allocation in Central Asia: leveraging decision support system. *Water*, 18(2), 161. https://doi.org/10.3390/w18020161

44. Conrad, C., Usman, M., Morper-Busch, L., Schönbrodt-Stitt, S. (2020). Remote sensing-based assessments of land use, soil and vegetation status, crop production and water use in irrigation systems of the Aral Sea Basin: a review. *Water Security*, 11, 100078. https://doi.org/10.1016/j.wasec.2020.100078

45. Ragettli, S., Kreiner, A., Yakovlev, A., et al. (2025). Unraveling agricultural water use in three Central Asian irrigation oases using remote sensing. *Journal of Hydrology: Regional Studies*, 59, 102414. https://doi.org/10.1016/j.ejrh.2025.102414

46. Hu, Z., Zhang, Z., Sang, Y.-F., et al. (2021). Temporal and spatial variations in the terrestrial water storage across Central Asia based on multiple satellite datasets and global hydrological models. *Journal of Hydrology*, 596, 126013. https://doi.org/10.1016/j.jhydrol.2021.126013